Clay Minerals, (2016) **51**, 675–689

Al-free di-trioctahedral substitution in chlorite and a ferri-sudoite end-member

VINCENT TRINCAL[1,*,†] AND PIERRE LANARI[2]

[1] *Laboratoire Chrono-Environnement, UMR CNRS 6249, University of Bourgogne Franche-Comté, 16 Route de Gray, F-25000 Besançon, France*

[2] *Institute of Geological Sciences, University of Bern, Baltzestrasse 1+3, CH-3012 Bern, Switzerland*

(*Received 01 November 2015; revised 30 April 2016; Guest editor: Atsuyuki Inoue*)

ABSTRACT: A compilation of Fe^{3+}-bearing chlorite analyses is used: (1) to investigate the Al-free di-trioctahedral (AFDT) substitution $2Fe^{3+} + \square = 3(Mg,Fe^{2+})$ in chlorite; and (2) to estimate the composition of a ferri-sudoite end-member $(Si_3Al)[(Fe^{2+},Mg)_2Fe_2^{3+}\square Al]O_{10}(OH)_8$ within the chlorite solid-solution domain. According to our observations, up to two Fe^{3+} cations might be allocated in the M2-M3 chlorite sites by the substitution AFDT, which does not involve Al. These unexpected observations were made possible by the development of μXANES techniques allowing *in situ* measurements of XFe^{3+} ($Fe^{3+}/(Fe^{2+} + Fe^{3+})$) in heterogeneous chlorite. Although further studies are required to confirm the crystallographic position of Fe^{3+} and refine its ionic/magnetic behaviour in chlorite, this development creates opportunities for developing new geothermometers.

KEYWORDS: chlorite, μXANES, geothermometry, sudoite.

Chlorite is a ubiquitous phyllosilicate composed of tetrahedral and octahedral layers according to the 14.2 Å 2:1:1 arrangement (*e.g.* Meunier, 2005). The tetrahedral sheet hosts tri- or tetravalent cations (Si^{4+}, Al^{3+} or rarely Ti^{4+}, Fe^{3+}), while the octahedral one is composed of di- or trivalent cations (usually Fe^{2+}, Mg^{2+}, Mn^{2+}, Al^{3+} and Fe^{3+}). The general formula of chlorite is: $R^{2+}_{6-x-3y}R^{3+}_{x+2y}\square_y(Si_{4-x}R^{3+}_x)O_{10}(OH)_8$, in which R^{2+} represents divalent cations, R^{3+} trivalent cations and $\square$ octahedral vacancies (*e.g.* Wiewióra & Weiss, 1990). According to Bailey (1988), the chlorite structure is formed of two types of tetrahedral crystallographic sites (denoted T1 and T2) and two octahedral sites (denoted M1 and M2). Two other octahedral sites (M3 and M4) are located in the brucite interlayer space. Al^{VI} or trivalent Fe^{3+} cations are located preferentially in the M4 site, while the divalent cations occupy the other sites (Bailey, 1988). There are three categories of chlorite in diagenetic and low- to high-grade metamorphic rocks: tri-trioctahedral (sum of octahedral cations close to 6 a.p.f.u), di-trioctahedral (5 a.p.f.u) and di-dioctahedral (4 a.p.f.u). The main chemical substitutions occurring in chlorite are: Tschermak (TK) $Si^{4+}_{(IV)} + (Fe^{2+}, Mg^{2+})_{(VI)} = Al^{3+}_{(IV)} + Al^{3+}_{(VI)}$; ferromagnesian (FM) $Mg^{2+}_{(VI)} = Fe^{2+}_{(VI)}$ and di-trioctahedral (DT) $2Al^{3+}_{(VI)} + \square_{(VI)} = 3(Mg^{2+},Fe^{2+})_{(VI)}$. Two filling models are used in the literature for the distribution of cations on the crystallographic sites. The first model referred to as 'disorderly', considers that there is no preferred configuration (*e.g.* Inoue *et al.*, 2009). The second model, referred to as 'ordered' is constrained by specific rules for filling cations in the crystallographic sites such as preferred configuration and Fe-Mg equipartition (*e.g.* Vidal *et al.*, 2001, 2005, 2006; Lanari *et al.*, 2014a). These authors assume, following Holland *et al.* (1998), Al_{IV} in T2, vacancies in M1, Al_{VI}

*E-mail: vincenttrincal@gmail.com

† This work was originally presented during the session 'The many faces of chlorite', part of the Euroclay 2015 conference held in July 2015 in Edinburgh, UK.

DOI: 10.1180/claymin.2016.051.4.09

TABLE 1. Structural formulae for classic chlorite end-members and the new ferri-sudoite end-member.

	T1(2)	T2(2)	M1(1)	M2-M3(4)	M4(1)
Amesite-Mg/corundophilite	Si,Si	Al,Al	Al	Mg,Mg,Mg,Mg	Al
Amesite-Fe	Si,Si	Al,Al	Al	Fe,Fe,Fe,Fe	Al
Clinochlore	Si,Si	Si,Al	Mg	Mg,Mg,Mg,Mg	Al
Chamosite/daphnite	Si,Si	Si,Al	Fe	Fe,Fe,Fe,Fe	Al
Sudoite-Mg	Si,Si	Si,Al	□	Mg,Mg,Al,Al	Al
Sudoite-Fe	Si,Si	Si,Al	□	Fe,Fe,Al,Al	Al
Al-free chlorite	Si,Si	Si,Si	Mg	Mg,Mg,Mg,Mg	Mg
Pyrophyllite-gibbsite	Si,Si	Si,Si	□	Al,Al,Al,□	Al
Ferri-sudoite	Si,Si	Si,Al	□	$(Fe,Mg)_2,Fe^{3+},Fe^{3+}$	Al

The numbers in parentheses refer to the quantity of atoms (per structural formula) distributed in tetrahedral (T) or octahedral (M) sites.

in M4 then M1 and then, eventually, in M2-M3, Fe and Mg in M2-M3 then in M1. Following the equipartition assumption, *X*Mg ($Mg^{2+}/(Mg^{2+} + Fe^{2+})$) is considered to be equal between the M1 and M2-M3 sites. Several chlorite end-members are classically defined (Table 1): Al-free chlorite $(Si_4)[Mg_6]O_{10}(OH)_8$, amesite $(Si_2Al_2)[(Fe^{2+},Mg)_4Al_2]O_{10}(OH)_8$, clinochlore $(Si_3Al)[Mg_5Al)O_{10}(OH)_8$, corundophilite $(Si_2Al_2)[Mg_4Al_2]O_{10}(OH)_8$, daphnite $(Si_3Al)[Fe^{2+}_5Al]O_{10}(OH)_8$, pyrophyllite-gibbsite $(Si_4)[Al_4□_2]O_{10}(OH)_8$ and sudoite $(Si_3Al)[(Fe^{2+},Mg)_2□Al_3]O_{10}(OH)_8$. These end-members do not include any ferric iron component.

For 15 years, many authors have emphasized the importance of Fe^{3+} in chlorite, particularly in terms of its use as a geothermometer (Laird, 1988; Vidal *et al*., 2006; Inoue *et al*., 2009; Bourdelle *et al*., 2013; Lanari *et al*., 2014a). An additional substitution: Al-Fe^{3+} that is supposed to occur on the M4 site was defined but without defining a ferric chlorite end-member (Vidal *et al*., 2006). In this model, the incorporation of Fe^{3+} changes the chlorite composition and the activity of the other end-members. This choice of the M4 site is based on the results of Smyth *et al*. (1997) suggesting that Fe^{3+} in chlorite shows a strong preference for the M4 site where it substitutes for Al^{3+}.

Several methods are available to measure Fe^{3+} in chlorite: chemical titration (Tschermak, 1891; Orcel, 1927; Hallimond *et al*., 1939; Brindley, 1951), Mössbauer (Pal *et al*., 1993; Aja & Dyar, 2000; Inoue *et al*., 2009), X-ray photoelectron spectroscopy (XPS) (Inoue *et al*., 2010) and micro-X-ray absorption near-edge spectroscopy (μ-XANES) (Wilke *et al*., 2001; Vidal *et al*., 2006; Rigault, 2010; Trincal *et al*., 2015).

CHLORITE DATA FROM THE LITERATURE

A compilation of almost 200 published data of chlorite structural formulae containing Fe^{3+} is reported in Table 2. These chlorites come from a wide range of rocks from various localities. Some are of detrital origin; another experienced diagenetic to metamorphic conditions as indicated by the oscillatory zoned chlorites from the Pic-de-Port-Vieux outcrop (Fig. 1; Trincal *et al*., 2015). In addition, 202 data from three localities were incorporated in this review (Inoue *et al*., 2009). Most of the chlorites selected contain (in a.p.f.u, see Table 2): 2.5 to 3.5 Si^{4+}, 2 to 4 Al^{3+} (Fig. 2), 1.5 to 5.5 R^{2+} (Mg^{2+}, Mn^{2+}, Fe^{2+}) (Fig. 3) and <1 Fe^{3+} (Fig. 4). These analyses are distributed between classical end-members and apparently follow the classical DT and TK substitutions (Figs 2, 3) or the Al-Fe^{3+} substitution (Fig. 4).

In diagenetic to metamorphic rocks, the *X*Fe^{3+} content of chlorite depends on the temperature and the oxygen fugacity that is controlled by the buffering assemblage, *i.e.* the bulk-rock composition (Lanari *et al.* 2014a). This control is supported by data from Inoue *et al.* (2009), which show relationships between sampling localities and chlorite structural formulae and oxidation state (Figs 2–4). It is therefore critical to look at the variability of *X*Fe^{3+} recorded by chlorite in one rock sample, for a given bulk-rock composition. In such cases the observed variability of *X*Fe^{3+} is caused by temperature variations,

Compilation of structural formulae for Fe^{3+}-bearing chlorites, calculated on the basis of O = 14.

od	SiO_2	TiO_2	Al_2O_3	Fe_2O_3	FeO	MgO	MnO	CaO + Na_2O + K_2O	Others	Total	Si	Ti	^{IV}Al	^{VI}Al	Fe^{3+}	Fe^{2+}	Mg	Mn	□
	25.17	0.01	22.76		20.98	17.27	0.09	0.05	0.05	86.37	2.58		1.42	1.33	0.68	1.04	2.64		0.30
	26.11	0.01	22.93		18.43	19.64	0.09	0.04	0.05	87.29	2.63		1.37	1.35	0.38	1.13	2.95		0.18
	25.74	0.01	23.25		20.43	17.86	0.09	0.04	0.05	87.47	2.60		1.40	1.37	0.53	1.14	2.69		0.25
	25.98	0.01	23.65		18.39	19.09	0.09	0.04	0.05	87.30	2.62		1.38	1.42	0.32	1.19	2.87		0.18
	25.53	0.01	23.16		21.94	16.41	0.08	0.04	0.04	87.23	2.59		1.41	1.37	0.74	1.04	2.48		0.35
	25.76	0.02	22.91		21.92	16.36	0.10	0.05	0.05	87.17	2.62		1.38	1.37	0.70	1.08	2.48		0.35
	26.39	0.01	23.00		17.59	19.83	0.11	0.05	0.05	87.02	2.65		1.35	1.38	0.36	1.08	2.97		0.20
	25.75	0.02	23.17		20.47	17.44	0.11	0.05	0.05	87.04	2.62		1.38	1.39	0.53	1.15	2.64		0.27
	25.85	0.01	23.55		18.70	18.83	0.11	0.05	0.05	87.15	2.61		1.39	1.42	0.33	1.22	2.84		0.18
	25.55	0.02	23.05		21.48	16.58	0.11	0.05	0.05	86.87	2.60		1.40	1.37	0.72	1.02	2.52		0.35
	33.76		12.69		4.17	33.65			1.59	86.14	3.23		0.77	0.66	0.20	0.14	4.80		0.04
	33.73		13.54		3.35	33.92			1.40	87.00	3.19		0.81	0.70	0.17	0.16	4.79		0.03
	33.47		13.24		3.26	33.66			1.76	85.57	3.21		0.79	0.71	0.13	0.13	4.81		0.02
											2.67	0.01	1.33	1.24	0.47	1.51	2.75	0.01	0.19
	29.98		15.56	6.36	16.45	16.68	0.40	0.33		85.75	3.13		0.87	1.05	0.50	1.44	2.60	0.04	0.33
	28.08	0.07	18.34	3.80	13.82	19.08	1.12	0.31		84.60	2.93	0.01	1.07	1.18	0.30	1.21	2.97	0.10	0.19
	27.34	0.03	18.58	4.51	16.42	17.75	0.35	0.27		85.24	2.87	0.00	1.13	1.17	0.36	1.44	2.78	0.03	0.18
	29.98	0.04	19.05	3.91	11.26	20.30	0.60	0.29		84.45	3.03	0.00	0.97	1.30	0.30	0.95	3.06	0.05	0.30
	24.26	0.01	17.64	5.56	33.82	1.37	3.34	0.11		86.09	2.85	0.00	1.15	1.29	0.49	3.32	0.24	0.33	0.31
	27.17	0.05	18.77	3.76	19.37	13.71	3.21	0.24		86.29	2.89	0.00	1.11	1.25	0.30	1.73	2.18	0.29	0.21
	22.86	0.03	17.55	6.40	30.55	1.92	2.15	0.13		81.59	2.80	0.00	1.20	1.33	0.59	3.13	0.35	0.22	0.35
											2.63	0.01	1.36	1.41	0.13	2.51	1.84	0.01	0.08
											2.71		1.29	1.60	0.14	2.58	1.40	0.05	0.22
											2.92		1.08	1.62	0.10	1.82	2.11	0.02	0.31
											2.86		1.14	1.44	0.34	0.34	3.54		0.32
											2.78	0.01	1.21	1.10	0.79	0.79	2.94	0.03	0.34
											2.57	0.01	1.42	1.29	0.75	1.84	1.79	0.01	0.30
											2.93		1.07	1.53	0.18	0.39	3.57		0.32
											2.67	0.03	1.31	0.33	1.74	1.51	2.22	0.01	0.38
											2.76		1.24	1.37	0.49	2.14	1.62		0.31
											2.72		1.28	1.32	0.43	2.11	1.85		0.24
											2.71		1.29	1.31	0.14	2.58	1.84		0.07

(continued)

od	SiO_2	TiO_2	Al_2O_3	Fe_2O_3	FeO	MgO	MnO	CaO + Na_2O + K_2O	Others	Total	Si	Ti	^{IV}Al	^{VI}Al	Fe^{3+}	Fe^{2+}	Mg	Mn	□
											2.69		1.31	1.31	0.14	2.60	1.82		0.07
	30.70	0.25	22.90	1.42		31.10	0.01	<0.20	0.01		2.88		1.12	1.41	0.01	0.10	4.35		0.15
	33.60	0.11	13.70	5.95		32.90	0.13	<0.74	0.01		3.24		0.76	0.78	0.13	0.30	4.73		0.07
	26.15		21.13	5.93	17.20	17.73				88.14	2.67		1.33	1.21	0.46	1.47	2.70		0.17
	26.83		21.64	6.07	13.30	20.67				88.51	2.67		1.33	1.21	0.45	1.11	3.07		0.17
	29.64	0.04	23.93		37.94	8.11	0.29	0.05	0.01		2.82		1.19	1.49	0.30	2.72	1.15	0.03	0.30
	33.90	0.06	23.77		8.33	33.80	0.04	0.10	0.01		2.83		1.17	1.17	0.07	0.50	4.20	0.01	0.03
	26.73	1.92	20.21		41.25	7.00	0.29	1.49	1.11		2.63	0.14	1.23	1.11	0.28	3.08	1.03	0.03	0.08
	37.02		35.61	0.89		11.07	0.07	1.20			3.23		0.77	3.11	0.03	0.02	1.65		1.19
	36.70		33.04	3.74		11.04		0.65			3.32		0.68	2.93	0.15	0.13	1.58		1.20
	36.81		30.58	7.25		8.13	0.11	1.14			3.42		0.58	2.87	0.33	0.24	1.24	0.01	1.31
	22.46	0.06	19.29	4.70	37.20	2.87	0.07			86.65	2.62	0.01	1.38	1.28	0.41	3.63	0.50	0.01	0.16
	30.38	0.10	18.70	0.79	6.29	29.81	0.05			86.12	2.94	0.01	1.06	1.08	0.06	0.51	4.30	0.00	0.04
											2.68		1.32	1.18	0.18	1.95	2.68		0.02
	27.69	0.02	22.26		12.26	24.56	0.17	0.01	0.08	87.05	2.73	0.00	1.27	1.32	0.37	0.64	3.61	0.01	0.22
	26.74	0.06	21.77		11.72	24.36	0.17	0.01	0.17	85.00	2.70	0.01	1.29	1.31	0.37	0.62	3.67	0.02	0.19
	27.42	0.05	22.11		12.28	24.72	0.15	0.01	0.16	85.67	2.72	0.00	1.28	1.30	0.38	0.64	3.65	0.01	0.20
	31.68	0.05	17.13	1.34	1.62	34.76	0.08		0.05		2.99	0.00	1.01	0.89	0.10	0.13	4.88	0.01	0
											3.50		0.50	0.70	0.10	0.10	4.90		0.15
											3.00		1.00	0.90	0.10	0.10	4.90		0
											3.12		0.88	1.69	0.64	1.03	2.17		0.73
											3.01		0.99	0.49	0.29	0.50	4.20		0
											2.76		1.24	2.01	0.12	0.70	3.30		0.45
	27.69	0.02	22.26		12.26	24.56	0.17	0.01	0.08	87.05	2.73	0.00	1.27	1.32	0.38	0.63	3.61	0.01	0.21
	26.74	0.06	21.77		11.72	24.36	0.17	0.01	0.17	85.00	2.70	0.00	1.29	1.30	0.37	0.62	3.67	0.01	0.19
	27.42	0.05	22.11		12.28	24.72	0.15	0.01	0.16	86.90	2.71	0.00	1.29	1.30	0.38	0.64	3.65	0.01	0.19
	35.70		33.77	2.81	0.35	13.26	0.04		0.06	86.00	3.24		0.76	2.85	0.19	0.03	1.79		1.14
	39.25	0.48	32.94	2.98		9.49		0.26	0.02		3.54	0.03	0.43	3.07	0.20		1.28		1.41
	24.40		21.14		32.65	11.74	0.07				2.59		1.41	1.24	0.16	2.73	1.86	0.01	0
											2.85		1.15	0.97	0.18	0.28	4.55		0.00
											2.96		1.04	0.54	0.23	0.09	4.73		0
											2.83		1.17	4.32	0.07				1.61
											2.88		1.12	1.32	0.23	2.07	2.16	0.05	0.22
											2.68		1.32	1.06	0.14	1.44	3.06	0.07	0
											2.64		1.36	0.85	0.32	1.82	3.10		0

											2.69		1.31	1.55		0.86	3.47		0.12
											2.62		1.38	1.28	0.14	1.16	2.96		0.02
											2.64		1.36	1.08	0.92	2.75	0.93		0.32
											2.97	0.35	0.68	1.85	0.33	2.41	0.83		0.75
											2.68		1.32	1.18	0.18	1.95	2.69		0.02
											3.00		1.00	0.96	0.14	0.48	4.30		0.05
32.90	0.06	35.40	2.69		14.73	0.01	0.01		0.07		3.00		1.00	2.81	0.18		2.00		1.00
20.95		35.21		8.28	22.88		0.58			88.90	2.01		1.99	2.00		0.66	3.28		0.00
21.42	0.26	34.06	0.63	0.95	28.66		0.51			86.49	2.02	0.02	1.98	1.82	0.04	0.08	4.04		0
											2.68		1.32	1.17	0.18	1.95	2.69		0.02
											2.97		1.03	1.44	0.07	0.99	3.24		0.24
											2.97		1.03	1.44	0.07	0.99	3.24		0.24
											2.99		1.01	1.39	0.21	0.57	3.52		0.30
											2.47		1.53	1.60		3.29	1.05		0.04
											2.84		1.16	1.75	0.12	2.61	1.16		0.36
33.55		22.62	2.51	15.74	25.58	–					2.91		1.09	1.23	0.16	1.14	3.31		0.15
25.89		19.85	12.61	30.57	4.77	6.31					2.61		1.39	0.96	0.95	2.57	0.72	0.54	0.26
30.66		22.69	14.58	25.48	5.50	1.09					2.89		1.11	1.42	1.04	2.01	0.77	0.09	0.67
32.81	0.18	35.71	2.66	1.07	13.54	0.29	0.06				2.99	0.01	1.00	2.85	0.18	0.08	1.84	0.02	1.01
											3.03		0.97	2.86	0.14	0.14	1.89	0.03	1.01
											3.04		0.96	2.87	0.13	0.14	1.88	0.04	1.02
32.20	0.03	15.23		1.19	35.56				3.40		3.02		0.98	0.72	0.04	0.04	4.95		0
31.58	0.04	15.37		1.42	34.93				3.57		2.99		1.01	0.71	0.06	0.06	4.92		0
											2.85	0.09	1.07	1.26	0.08	0.26	4.24		0.14
											3.12		0.89	0.60	0.18	0.32	4.95		0
											2.81		1.20	1.01	3.02	0.64	0.79	0.33	1.42
											3.12		0.88	1.47	0.13	3.18	0.73	0.12	0.35
33.06		35.74	2.74	0.24	14.09	0.28					3.01		0.99	2.84	0.19	0.02	1.91	0.02	1.02
32.82		36.16	2.45	0.05	14.35	0.24					2.99		1.01	2.86	0.17		1.94	0.02	1.01
34.36		38.34	0.49		10.21		0.25				3.12		0.88	3.29	0.03		1.39		1.16
35.67	0.19	37.41	0.20	0.09	11.97	0.02	1.25				3.18	0.01	0.81	3.12	0.01	0.01	1.59		1.12
33.71		37.95	2.74	2.40	12.08		1.49				2.97		1.03	2.90	0.18	0.17	1.58		1.03
36.07		32.42	1.99		15.94		0.44				3.24		0.76	2.67	0.13		2.14		0.99
33.83	0.34	31.80	0.27	0.37	18.86		2.42				3.04	0.03	0.93	2.43	0.03	0.04	2.50		0.77
											2.95		1.05	0.46	0.08	0.07	2.39		0
											2.82		1.19	0.55	0.53	1.59	2.60	0.04	0

(continued)

od	SiO_2	TiO_2	Al_2O_3	Fe_2O_3	FeO	MgO	MnO	CaO + Na_2O + K_2O	Others	Total	Si	Ti	^{IV}Al	^{VI}Al	Fe^{3+}	Fe^{2+}	Mg	Mn	□
											2.54		1.46	0.90	1.13	2.60	1.10		0.28
											2.49		1.51	1.51	0.61	2.53	0.71	0.25	0.31
											2.54	0.05	1.41	1.05	0.54	2.19	2.00	0.12	0.09
											2.55		1.45	1.37	0.33	1.50	2.65	0.03	0.13
											3.19		0.81	3.13	0.01	0.01	1.60		1.13
	34.36		38.84	0.49		10.21		0.85		85.75	3.12		0.88	3.29	0.03		1.38		1.16
	38.26		44.28	1.31	0.48				2.00		3.42		0.58	4.08	0.09	0.04			1.79
	33.10	0.30	37.43	0.87		13.12		0.44		85.26	3.01	0.02	0.97	3.05	0.06		1.78		1.04
	29.45	0.20	20.14	4.08	18.69	14.93	0.36	1.59		89.34	2.97	0.02	1.02	1.36	0.31	1.58	2.24	0.03	0.27
	30.84	0.12	14.15	2.59	18.42	20.62	0.10	0.84		87.68	3.15	0.01	0.84	0.87	0.20	1.58	3.14	0.01	0.09
	25.80		18.30	4.10	21.30	20.30				89.80	2.64		1.36	0.85	0.32	1.82	3.10		0
	27.90		25.20		10.60	24.20				87.90	2.69		1.31	1.55		0.85	3.48		0.12
	30.50		17.30	2.90	6.10	32.80				89.60	2.87		1.13	0.79	0.21	0.48	4.60		0
	33.90		14.60	2.70	2.10	34.60				87.90	3.16		0.84	0.77	0.19	0.16	4.81		0.06
											3.14		0.86	4.10	0.04	0.01	0.08		1.64
	27.27		15.21	4.35	2.78	10.13	0.06	0.28	29.87	89.98	2.99		1.01	0.95	0.36	0.25	1.65	0.01	0.15
	27.27		15.21	4.35	2.78	10.13	0.06	0.38	29.87		2.98		1.02	0.95	0.36	0.25	1.65	0.01	0.14
	32.72	0.03	20.28	1.00		24.47	0.06	2.22		80.78	3.24	0.00	0.76	1.61	0.07		3.61	0.01	0.44
	31.17		37.49	1.04	1.95	14.25		0.26			2.85		1.15	2.90	0.07	0.15	1.95		0.91
											3.45		0.55	3.96	0.02	0.02	0.04	0.01	1.72
											2.66		1.34	1.74	0.02	3.68	0.42		0.21
											3.43		0.57	2.70	0.09	0.04	1.97		1.11
	27.31	0.22	19.69	3.23	18.58	19.01	0.27	0.80		89.11	2.78	0.02	1.20	1.16	0.25	1.58	2.88	0.02	0.11
	35.63		34.87	5.01	0.43	8.63	0.05	1.83		86.45	3.26		0.74	3.02	0.34	0.04	1.17		1.31
	39.01	0.47	32.15	0.90	0.10	10.14		2.16			3.56	0.03	0.41	3.05	0.06	0.01	1.37		1.25
	30.66		30.55	0.47		10.13		1.79			3.24		0.76	3.04	0.04		1.59		1.00
	24.45	0.21	21.99	20.80	28.04	11.90	0.54	0.25		89.46	2.59	0.02	1.39	1.36	0.17	2.19	1.88	0.05	0.06
											2.70		1.30	4.30	0.03	0.02			1.52
											2.80	0.09	1.11	3.31	0.38		0.76		1.18
	28.32	0.09	19.03	1.19	14.85	23.72	0.09	0.63		87.92	2.83	0.01	1.17	1.06	0.09	1.24	3.53	0.01	0
	21.34	0.21	20.73	5.20	40.17	0.99	0.89	0.04		89.57	2.46	0.02	1.52	1.30	0.45	3.87	0.17	0.09	0.12
	36.43		12.24	0.94	6.87	30.94	0.11	0.33	0.63	88.49	3.43		0.57	0.79	0.07	0.54	4.35	0.01	0.15
	33.14	0.08	10.04	4.00	5.66	32.64		0.80		86.36	3.25	0.01	0.75	0.41	0.29	0.46	4.77		0
	29.73		17.95	0.68	10.05	21.84	8.24			88.49	2.98		1.02	1.09	0.05	0.84	3.26	0.70	0.06
	22.81		20.35	4.84	34.87	6.11	0.56	0.10			2.54		1.46	1.20	0.40	3.24	1.01	0.05	0.07

23.38		19.32	2.51	38.38	5.39	0.58				89.56	2.63		1.37	1.20	0.21	3.61	0.90	0.06	0.02
26.04		19.96	1.85	21.34	18.56	0.47				88.22	2.69		1.31	1.13	0.14	1.85	2.86	0.04	0
29.71		19.75	0.29	6.59	30.79	0.30				87.43	2.84		1.16	1.07	0.02	0.53	4.39	0.02	0
32.27		14.99	1.56	6.89	31.75	0.09				87.55	3.10		0.90	0.79	0.11	0.55	4.54	0.01	0.00
27.11	0.35	17.42	2.91	30.98	9.75		0.21			88.73	2.93	0.03	1.07	1.15	0.24	2.80	1.57		0.16
29.94	0.16	13.77	10.46	20.96	10.71	0.18	1.34			87.52	3.19	0.01	0.81	0.92	0.84	1.87	1.70	0.02	0.45
28.73	0.41	19.16	1.97	10.99	26.37	0.15	0.10			87.88	2.81	0.03	1.19	1.03	0.15	0.90	3.85	0.01	0
22.47		21.82	0.22	37.24	2.57					84.32	2.65		1.35	1.68	0.02	3.67	0.45		0.18
23.48		22.45	43.37	0.45	2.60					92.35	2.35		1.65	1.00	3.27	0.04	0.39		1.31
33.40		47.47		0.71	0.20		0.54		3.12	85.44	3.07		0.93	4.22		0.05	0.03		1.64
29.84	0.15	20.20	0.80	15.00	21.83	0.13	0.80		0.03	88.78	2.93	0.01	1.07	1.27	0.06	1.23	3.19	0.01	0.12
22.03	3.63	22.91	0.46	36.68	1.91	0.04	0.18		0.26	88.77	2.47	0.31	1.53	1.50	0.04	3.44	0.32	0.00	0
											3.10		0.90	1.30	0.60	3.35	0.75		0.50
											2.48	0.30	1.22	1.82	0.04	3.46	0.32		0.32
21.40	0.89	25.40	0.25	37.60	2.04	0.05	0.13			87.98	2.42	0.08	1.58	1.80	0.02	3.55	0.34	0.00	0.12
											2.48	0.30	1.22	1.82	0.04	3.46	0.32		0.32
26.40		18.23	5.70	25.87	11.35	0.04	0.76			88.35	2.83		1.17	1.13	0.46	2.32	1.81	0.00	0.18
27.64	0.22	22.48	0.06	12.06	24.32	0.02	0.23		0.06	87.09	2.73	0.02	1.27	1.34	0.00	0.99	3.57	0.00	0.01
31.87	0.17	14.51	1.86	3.57	32.76		0.06		1.38	86.18	3.07	0.01	0.93	0.72	0.14	0.29	4.71		0
20.82		17.64	8.70	37.96	4.15					89.27	2.42		1.58	0.83	0.76	3.69	0.72		0.00
26.65		16.14	6.69	34.43	4.47					88.38	2.99		1.01	1.12	0.56	3.23	0.75		0.34
22.47		23.57	4.01	29.27	9.81					89.13	2.42		1.58	1.40	0.32	2.63	1.57		0.07
26.45		20.88	2.82	21.06	16.84	0.44	0.47			88.96	2.71		1.29	1.24	0.22	1.81	2.57	0.04	0.06
											3.09		0.91	3.92	0.05		0.21		1.44
											3.06		0.94	3.88	0.08		0.23		1.40
											3.10		0.90	4.16	0.07		0.11		1.67
											2.80		1.20	0.86	0.60	3.56	0.78	0.04	0.13
24.35	0.04	20.21	2.13	36.27	5.57	0.48	0.10			89.15	2.70	0.00	1.30	1.35	0.18	3.37	0.92	0.05	0.12
24.90		15.60	7.20	35.00	4.60	0.40				87.70	2.86		1.14	0.97	0.62	3.36	0.79	0.04	0.22
25.07	0.12	19.78	3.50	35.80	1.11	0.50	2.15			88.03	2.85	0.01	1.15	1.50	0.30	3.40	0.19	0.05	0.24
25.09	0.05	18.94	9.60	25.66	9.80	0.02	0.49			89.65	2.68	0.00	1.32	1.06	0.77	2.29	1.56	0.00	0.24
22.18	0.04	20.04	7.35	35.23	3.79	0.02	0.49			90.60	2.51	0.00	1.49	1.18	0.63	3.33	0.64	0.00	0.15
26.69	0.30	19.57	3.49	21.80	16.23	0.30	0.17		0.13	88.68	2.76	0.02	1.24	1.15	0.27	1.89	2.50	0.03	0.09
27.56		24.47	3.85	10.51	20.86	1.80				89.05	2.68		1.32	1.48	0.28	0.85	3.02	0.15	0.22
25.62	0.88	21.19	3.88	21.55	15.28	0.35	0.16			88.91	2.64	0.07	1.36	1.22	0.30	1.86	2.35	0.03	0.08
23.32	0.03	17.45	4.09	38.90	4.54	0.01	0.24			88.58	2.68	0.00	1.32	1.05	0.35	3.74	0.78	0.00	0.04
23.43		18.21	4.49	36.30	5.41					87.84	2.68		1.32	1.13	0.39	3.47	0.92		0.10
24.60		19.10	3.12	29.04	13.10					88.96	2.64		1.36	1.06	0.25	2.61	2.10		0

(continued)

od	SiO_2	TiO_2	Al_2O_3	Fe_2O_3	FeO	MgO	MnO	CaO + Na_2O + K_2O	Others	Total	Si	Ti	^{IV}Al	^{VI}Al	Fe^{3+}	Fe^{2+}	Mg	Mn	□
	26.65		16.14	6.69	34.43	4.47				88.38	2.99		1.01	1.12	0.56	3.23	0.75		0.34
	30.30		18.25	2.64	3.98	32.66		0.03		88.24	2.87		1.13	0.90	0.19	0.32	4.61		0
	20.82		17.64	8.70	37.96	4.15				89.27	2.42		1.58	0.83	0.76	3.69	0.72		0.00
	22.27	0.08	21.40	0.67	43.01	2.35	0.05	0.15		90.33	2.54	0.01	1.46	1.41	0.06	4.10	0.40	0.00	0.00
	26.50	0.03	20.85	1.90	18.73	19.85	0.52			88.38	2.69	0.00	1.31	1.19	0.15	1.59	3.01	0.04	0.01
	25.35		22.06	18.97	8.36	15.06	0.08			89.88	2.52		1.48	1.11	1.42	0.70	2.24	0.01	0.53
	27.12		27.68	0.20	1.24	30.96	0.54			87.74	2.51		1.49	1.54	0.01	0.10	4.28	0.04	0.03
	25.04		20.10	2.05	35.40	4.28				86.87	2.83		1.17	1.51	0.17	3.34	0.72		0.25
	23.20		24.42	3.48	13.40	32.76		1.04		88.30	2.10		1.90	0.71	0.24	1.01	4.42		0
	27.78		24.30	1.43	0.35	32.71				86.57	2.61		1.39	1.29	0.10	0.03	4.58		0.00
	24.40		22.77	0.45		32.70	0.09	0.40		80.81	2.47		1.53	1.18	0.03		4.93	0.01	0
	33.24		11.07	2.26	25.11	16.51	0.41	1.36		89.96	3.42		0.58	0.77	0.18	2.16	2.53	0.04	0.16
	23.62		22.26		38.97	1.09	0.98	1.67		88.59	2.68		1.32	1.67		3.70	0.18	0.09	0.03
	33.83		12.95	2.25	3.02	34.94				86.99	3.21		0.79	0.65	0.16	0.24	4.94		0.01
	33.46		10.96	2.56	24.72	16.52	0.40	1.21		89.83	3.44		0.56	0.77	0.20	2.13	2.53	0.03	0.18

using chemical titration (CHE) or, for the past 20 years, using XANES (XAN), Mössbauer (MÖS) or XPS spectroscopies. Where
on is assumed.

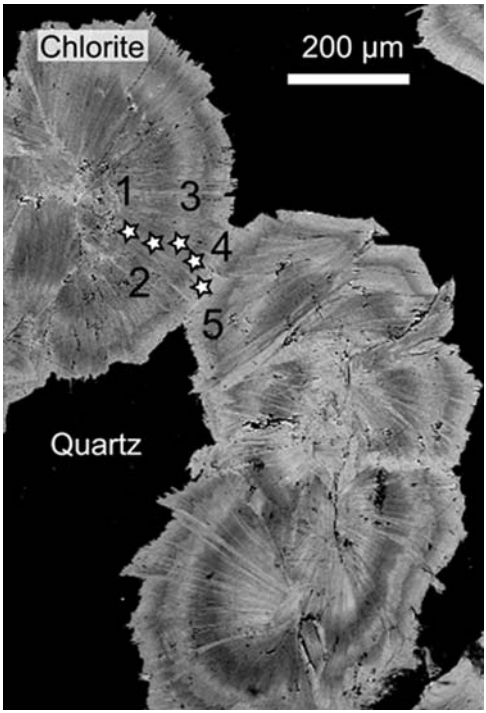

FIG. 1. Backscattered-electron image of an oscillatory-zoned chlorite showing Al-free di-trioctahedral substitution, from the Pic-de-Port-Vieux, Pyrenees, Spain. The numbers refer to the structural formulae reported in Table 2.

rather than by changes in the buffering assemblage (Lanari *et al.* 2014a; Trincal *et al.*, 2015). Most of the spot analyses reported in the literature correspond to different geological environments (Table 2); it is thus very difficult to use them to evaluate the link between the Fe^{3+} behaviour and the evolution of a parameter such as pressure, temperature, f_{O_2}, *etc*.

The choice of analytical method to estimate the XFe^{3+} in chlorite is essential. Chlorite Fe^{3+} measurements by Mössbauer spectroscopy or titration are relatively common but provide few constraints due to poor spatial resolution. Indeed, recent investigations using high-resolution mapping (*e.g.* de Andrade *et al.*, 2006; Muñoz *et al.*, 2006) have demonstrated that chlorite is frequently zoned, recording strong compositional variability even at the crystal scale (*e.g.* Lanari *et al.*, 2014b). Compositional zoning reflects time series of equilibrium conditions experienced by the rock. Thus *in situ* micrometric analyses are required to ensure a precise determination of the Fe^{3+}/Fe_{Tot} of the successive growth zones, which is impossible using Mössbauer spectroscopy. µ-XANES XFe^{3+} spot analyses or mapping allow us to elucidate the heterogeneity of the Fe chemistry of chlorite which is critical to see the relations between formation temperature and crystal geometry (Vidal *et al.*, 2006; Trincal *et al.*, 2015).

µXANES DATA FROM ZONED CHLORITES

Accurate *in situ* µXANES and electron microprobe analyses performed on zoned chlorite from the Sambagawa metamorphic belt in Japan (Vidal *et al.*, 2006) and on oscillatory-zoned chlorite from hydrothermal veins in the Pic-de-Port-Vieux, Pyrenees, Spain (fig. 1 from Trincal *et al.*, 2015) show variations in the composition of the Fe^{3+}, Mg and Fe^{2+} cation proportions, while that of Si and Al remain constant (Table 2, Fig. 2). This trend is observed independently in both samples, which have different bulk-rock compositions and experienced different metamorphic conditions. Indeed, chlorite from Japan comes from a blueschist-facies metapelite made of K-white mica, garnet, albite, quartz and graphite (Vidal *et al.*, 2006), while the chlorite from the Pyrenees crystallizes in a vein of a greenschist-facies metapelite without garnet or graphite (Trincal *et al.*, 2015). The absence of graphite is a good indicator of more oxidizing conditions. In both cases, XFe^{3+} increases as temperature decreases, as suggested by numerous authors (*e.g.* Lanari *et al.*, 2014a; Vidal *et al.*, 2016). Furthermore, in both cases, there is no significant change in the Al content of the zoned chlorite. This result excludes the hypothesis of DT, TK or Al-Fe^{3+} substitutions being at the origin of the XFe^{3+} variations.

AL-FREE DI-TRIOCTAHEDRAL SUBSTITUTION

Based on µXANES analyses performed on zoned chlorite by Vidal *et al.* (2006) and Trincal *et al.* (2015), and in agreement with the literature data (Table 2), we demonstrate that a di-trioctahedral substitution implying Fe^{3+} can be used to explain the variations of XFe^{3+} in natural chlorite:

$$2Fe^{3+} + \square = 3(Mg^{2+}, Fe^{2+}) \quad (1)$$

As this substitution does not explicitly involve any Al cations, it is named Al-free di-trioctahedral substitution (AFDT); it must not be confused with the Al-free chlorite end-member.

This substitution is similar to another couple suggested by Billault *et al.* (2002) and based on electron microprobe

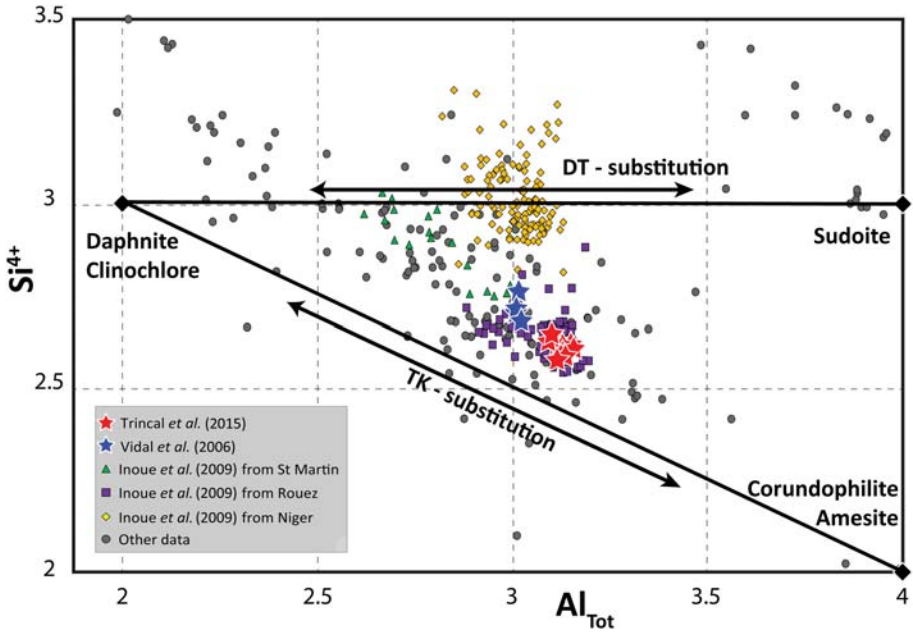

FIG. 2. Compilation of the Fe^{3+}-bearing chlorite compositions. The Si-Al plot is used to highlight the di-trioctahedral (DT) and Tschermak (TK) substitutions. End-members and structural formulae are reported in Tables 1 and 2.

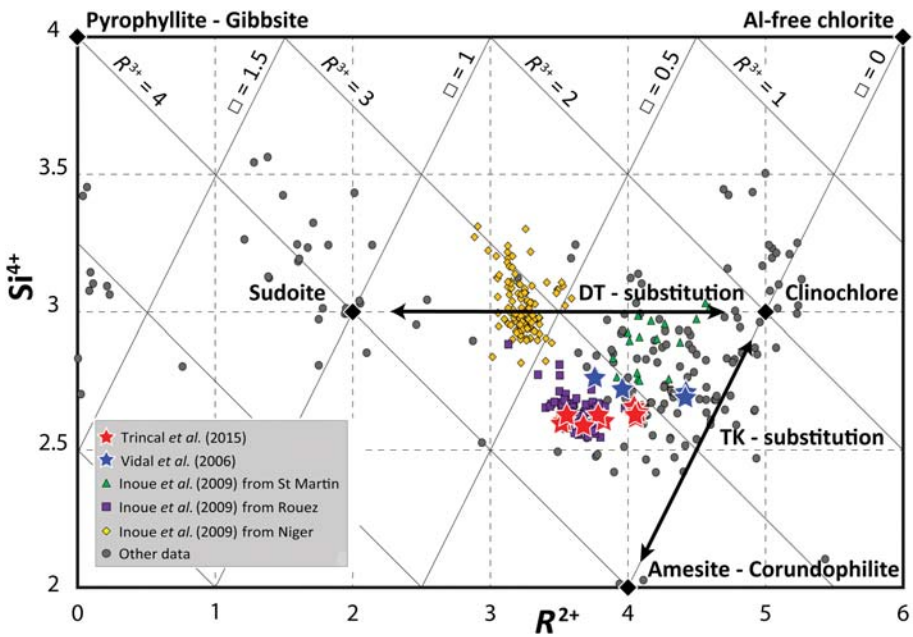

FIG. 3. Compilation of Fe^{3+}-bearing chlorite compositions. The $Si^{4+}-R^{2+}$ plot by Wiewióra & Weiss (1990) is used to highlight the di-trioctahedral (DT) and the Al-Fe^{3+} substitutions.

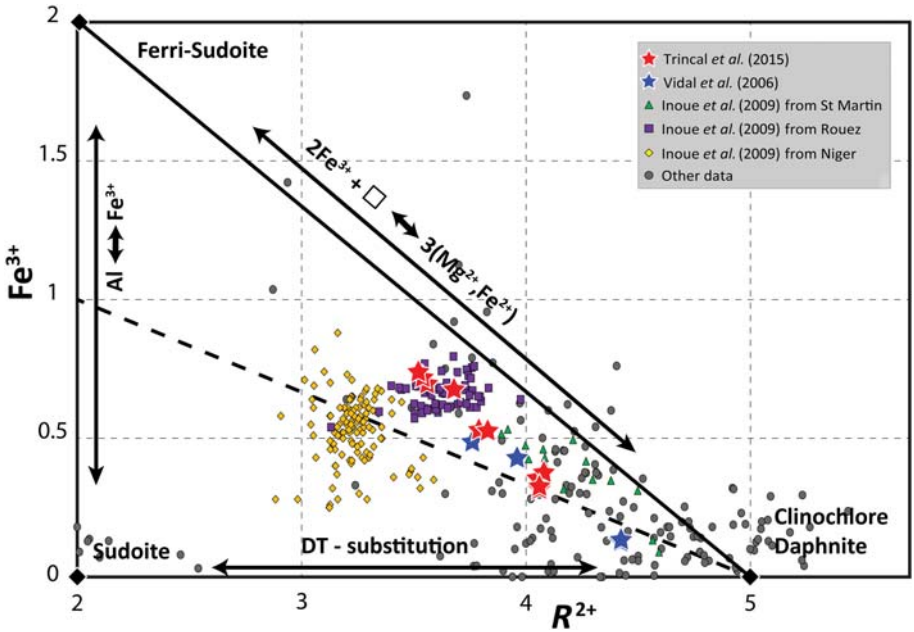

FIG. 4. Compilation of the Fe^{3+}-bearing chlorite compositions. The Fe^{3+}–R^{2+} plot highlights the di-trioctahedral (DT), Al-Fe^{3+} and AFDT substitutions.

and Mössbauer spectroscopic analyses on sudoite:

$$Fe^{3+} = Al_{(VI)} \text{ and } Fe^{2+} + Fe^{3+} + \square = 3(Mg^{2+}) \quad (2)$$

However, chlorite analyses from their study display both Al and *X*Mg variations, which is not the case for the samples in the present study.

Chlorite compositions from Vidal *et al.* (2006) and Trincal *et al.* (2015) are plotted in an Fe^{3+} *vs.* R^{2+} diagram (Fig. 4). In this diagram, data from zoned chlorite are distributed along a line parallel to the AFDT substitution vector. The AFDT substitution allows us to define a theoretical Fe^{3+}-bearing chlorite end-member; namely ferri-sudoite ($(Si_3Al)[(Fe^{2+},Mg)_2Fe^{3+}_2\square Al)O_{10}(OH)_8$) with two atoms of Fe^{3+} (Table 1). Ferri-sudoite can be separated into ferri-sudoite-Fe ($(Si_3Al)[Fe^{2+}_2Fe^{3+}_2\square Al)O_{10}(OH)_8$) and ferri-sudoite-Mg ($(Si_3Al)[Mg_2Fe^{3+}_2\square Al)O_{10}(OH)_8$). As Fe^{3+} replaces Mg and Fe^{2+}, it seems convenient to allocate up two atoms of Fe^{3+} to the M2-M3 sites (total multiplicity of 4) leaving Al in the M4 (Table 1).

According to several authors, the Fe^{3+} cation seems limited to 1 a.p.f.u and is generally allocated to the M4 site following the Al-Fe^{3+} substitution. This last assertion is supported by Z-contrast images of high-angle annular dark-field imaging-scanning transmission electron microscopy (HAADF-STEM) and other studies (*e.g.* Smyth *et al.*, 1997; Inoue & Kogure, 2016; Vidal *et al.*, 2016). Among data collected in the literature, only six analyses show Fe^{3+} contents of >1 a.p.f.u (Orcel, 1927; Brindley & Youell, 1953; Malysheva *et al.*, 1977; Goodman & Bain, 1979; Kodama *et al.*, 1982; Singer *et al.*, 2009 in Table 2). However, these analyses would actually match other phyllosilicates, suggesting contamination issues. Although AFDT substitution suggests that it is possible, no sudoite with >1 Fe^{3+} atom has been yet discovered; it offers interesting research opportunities.

CONCLUSION

The compilation of Fe^{3+}-bearing chlorite analyses in this study, especially those acquired by µXANES spectroscopy in zoned crystals, suggests the existence of a new chlorite substitution, the AFDT substitution that is characterized by $2Fe^{3+} + \square = 3(Mg^{2+}, Fe^{2+})$ and implies a new chlorite end-member: ferri-sudoite $(Si_3Al)[(Fe^{2+},Mg)_2Fe^{3+}_2\square Al)O_{10}(OH)_8$ with 2 atoms of Fe^{3+}. These results are not in agreement with previous studies which showed Al-Fe^{3+} substitution implying only 1 Fe^{3+}. The absence of constraints on the Fe^{3+} crystallographic position together with the Fe^{3+} ionic properties in chlorite require further studies to confirm

the existence of the AFDT substitution and of the ferri-sudoite end-member, *e.g.* with accurate *in situ* Fe^{3+} measurements in synthetic or diagenetic chlorite formed in different oxidizing environments. This study opens the door for further research developments that would have strong implications, *e.g.* in chlorite geothermometry.

ACKNOWLEDGEMENTS

The authors thank Daniel Beaufort, Olivier Vidal and Martin Engi for fruitful discussions regarding Fe^{3+} in chlorite; Atsuyuki Inoue, Fernando Nieto-Garcia and another referee for the valuable advice about the manuscript; and Flavien Choulet for corrections to the language.

REFERENCES

Ahn J.H. & Buseck P.R. (1988) Al-chlorite as a hydration reaction product of andalusite. *Mineralogical Magazine*, **52**, 396–399.

Aja S.U. & Dyar D.M. (2002) The stability of Fe–Mg chlorites in hydrothermal solutions—I. Results of experimental investigations. *Applied Geochemistry*, **17**, 1219–1239.

Aleksandrova V.A., Drits V.A. & Sokolova G.V. (1972) Structural features of dioctahedral one-packet chlorite. *Soviet Physics–Crystallography*, **17**, 456–461.

Alysheva E.I., Rusinova O.V. & Chekvaidze V.B. (1977) On sudoites from the polymetal deposits of Rydnyy Altai. *Doklady Academii Nauk SSSR*, **236**, 722–724.

Anceau A. (1992) Sudoite in some Visean (lower Carboniferous) K-bentonites from Belgium. *Clay Minerals*, **27**, 283–292.

Bailey S.W., editor (1988) *Hydrous Phyllosilicates (exclusive of Micas)*. Reviews in Mineralogy, **19**, Mineralogical Society of America, Washington, D.C.

Ballet O., Coey J.M.D. & Burke K.J. (1985) Magnetic properties of sheet silicates; 2: 1: 1 layer minerals. *Physics and Chemistry of Minerals*, **12**, 370–378.

Bannister F.A. & Whittard W.F. (1945) A magnesian chamosite from the Wenlock Limestone of Wickwar, Gloucestershire. *Mineralogical Magazine*, **27**, 99–111.

Banno S. (1964) Petrologic studies on Sanbagawa crystalline schists in the Bessi-Ino district, central Sikoku, Japan. *Journal of Faculty Science, University of Tokyo, Section II*, **15**, 203–319.

Battey M.H. (1956) The petrogenesis of a spilitic rock series from New Zealand. *Geological Magazine*, **93**, 89–110.

Bertoldi C., Benisek A., Cemic L. & Dachs E. (2001) The heat capacity of two natural chlorite group minerals derived from differential scanning calorimetry. *Physics and Chemistry of Minerals*, **28**, 332–336.

Bilgrami S.A. & Howie R.A. (1960) The mineralogy and petrology of a rodingite dike, Hindubagh, Pakistan. *American Mineralogist*, **45**, 791–801.

Billault V., Beaufort D., Patrier P. & Petit S. (2002) Crystal chemistry of Fe-sudoites from uranium deposits in the Athabasca basin (Saskatchewan, Canada). *Clays and Clay Minerals*, **50**, 70–81.

Borggaard O.K., Lindgreen H.B. & Morup S. (1982) Oxidation and reduction of structural iron in chlorite at 480°C. *Clays and Clay Minerals*, **30**, 353–364.

Bourdelle F., Benzerara K., Beyssac O., Cosmidis J., Neuville D.R., Brown G.E. Jr. & Paineau E. (2013) Quantification of the ferric/ferrous iron ratio in silicates by scanning transmission X-ray microscopy at the Fe L2,3 edges. *Contributions to Mineralogy and Petrology*, **166**, 423–434.

Brandt F., Bosbach D., Krawczyk-Bärsch E., Arnold T. & Bernhard G. (2003) Chlorite dissolution in the acid pH range: a combined microscopic and macroscopic approach. *Geochimica et Cosmochimica Acta*, **67**, 1451–1461.

Brindley G.W. (1951) The crystal structure of some chamosite minerals. *Mineralogical Magazine*, **29, 502–522**.

Brindley G.W. & Youell R.F. (1953) Ferrous chamosite and ferric chamosite. *Mineralogical Magazine*, **30**, 57–70.

Brydon J.E., Clark J.S. & Osborne V. (1961) Dioctahedral chlorite. *The Canadian Mineralogist*, **6**, 595–609.

Caillère S., Hénin S. & Pobeguin T. (1962) Présence d'un nouveau type de chlorite dans les 'bauxites' de Saint-Paul-de-Fenouillet (Pyrénées orientales). *Compte Rendu de l'Adadémie des Sciences*, **254**, 1657–1658.

Chamberlain S.C., Robinson G.W. & Richards R.P. (1989) Mineralogy of the Alpine veins near Sherbrooke, Quebec. *Mineralogical Record*, **20**, 209–20.

Chernykh V.V. (1926) Physicochemische Untersuchung der Serpentine und Chlorite. *Mémoire de la Société Russe de Minéralogie Série 2*, **55**, 183–194.

Dana E.S. (1915) *Descriptive Mineralogy.* John Wiley & Sons, New York, 659 pp.

De Andrade V., Vidal O., Lewin E., O'Brien P. & Agard P. (2006) Quantification of electron microprobe compositional maps of rock thin sections: an optimized method and examples RID C-2856–2009. *Journal of Metamorphic Geology*, **24**, 655–668.

Debret B., Bolfan-Casanova N., Padrón-Navarta J.A., Martin-Hernandez F., Andreani M., Garrido C.J., Sánchez-Vizcaíno V.L., Gómez-Pugnaire M.T., Muñoz M. & Trcera N. (2015) Redox state of iron during high-pressure serpentinite dehydration. *Contributions to Mineralogy and Petrology*, **169**, 1–18.

De Grave E., Vandenbruwaene J. & Bockstael M.V. (1987) ^{57}Fe Mössbauer spectroscopic analysis of chlorite. *Physics and Chemistry of Minerals*, **15**, 173–180.

De Waal S.A. (1970) Nickel minerals from Barberton, South Africa: III. Willemseite, a nickel-rich talc. *American Mineralogist*, **55**, 31–42.

Drits V.A. & Lazarenko E.K. (1967) Structural and mineralogical characteristics of donbassites. *Mineral Sb Lvov*, **21**, 40–48.

Dschang G. (1931) *Die Beziehungen Zwischen Chemischer Zusammensetzung und den Physikalisch-Optischen Eigenschaften in der Chloritgruppe.* Doctoral Dissertation Thesis, Fischer.

Engelhardt W.V. (1942) Die Strukturen von Thuringit, Bavalit und Chamosit und ihre Stellung in der Chloritgruppe. *Zeitschrift für Kristallographie-Crystalline Materials*, **104**, 142–159.

Ericsson M.T., Wäppling D.R. & Punakivi M.K. (1977) Mössbauer spectroscopy applied to clay and related minerals. *Geologiska Föreningen i Stockholm Förhandlingar*, **99**, 229–244.

Fransolet A.M. & Bourguignon A. (1978) Di/trioctahedral chlorite in quartz veins from the Ardennes, Belgium. *The Canadian Mineralogist*, **16**, 365–373.

Frenzel G. & Schembra F.W. (1965) Ein dioktaedrischer chlorit vom Kaiserbachtal (Südpfalz). *Neues Jahrbuch für Mineralogie Monatshefte*, **1965**, 108–114.

Frondel C. (1955) Two chlorites: gonyerite and melanolite. *American Mineralogist*, **40**, 1090–1094.

Ginzburg A.I. (1953) On lithium chlorite-cookeite. *Doklady Akademii Nauk SSSR*, **90**, 871.

Gomes C.S.F. (1967) Alteration of spodumene and lepidolite with formation of dioctahedral chlorite plus dioctahedral chlorite-dioctahedral montmorillonite interstratifications. *Publ Museu e Laboratorio Mineralogico e Geologico, Universidade de Coimbra, (Portugal), Memorias Noticias*, **64**, 32–57.

Goodman B.A. & Bain D.C. (1979) Mössbauer spectra of chlorites and their decomposition products, Pp. 65–74 in: *Developments in Sedimentology*, Vol. **27** (M.M. Mortland and V.C. Farmer, editor). Elsevier, Amsterdam.

Gregori D.A. & Mercader R.C. (1994) Mössbauer study of some Argentinian chlorites. *Hyperfine Interactions*, **83**, 495–498.

Hallimond A.F., Harvey C.O. & Bannister F.A. (1939) On the relation of chamosite and daphnite to the chlorite group. *Mineralogical Magazine*, **25**, 441–465.

Hawes G.W. (1875) On diabantite, a chlorite occurring in the trap of the Connecticut valley. *American Journal of Science*, 454–457.

Hayashi H. & Oinuma K. (1965) Relationship between infrared absorption spectra in the region of 450–900 CM-1 and chemical composition of chlorite. *American Mineralogist*, **50**, 476.

Hödl A. (1942) Über Chlorite der Ostalpen. Ein Beitrag zur Systematik der Chlorite. *Neues Jahrbuch für Mineralogie, Beil. Bd*, **77**, 1–77.

Holland T., Baker J. & Powell R. (1998) Mixing properties and activity-composition and relationships of chlorites in the system MgO-FeO-Al_2O_3-SiO_2-H_2O. *European Journal of Mineralogy*, **10**, 395–406.

Holzner J. (1937) Beiträge zur kentnnis der varistischen gesteins-und mineralprovinz im Lahn-Dillgebiet. *Zeitschrift für Kristallographie, Mineralogie und Petrographie*, **49**, 168–215.

Honda S. (1975) Dioctahedral chlorite, closely associated with kaolinite from the Kamikita mine (Kuroko deposit). *Report of the Research Institute of Underground Resesarch Mining College Akita University*, **43**, 1–8.

Horikoshi E. (1965) Kuroko-type exhalative sedimentary mineral deposits. *Journal of the Mining Institution of Kyusyu*, **33**, 300–210.

Hutton C.O. (1938) *The Stilpnomelane Group of Minerals.* Oxford University Press, Oxford, UK.

Hutton C.O. (1940) *Metamorphism in the Lake Wakatipu Region* (E.V. Paul, editor). Government Printer, Western Otago, New Zealand, 90 pp.

Hutton C.O. & Seelye F.T. (1945) Contributions to the mineralogy of New Zealand – Part I. Pp. 160–168 in: *Transactions of the Royal Society of New Zealand*, vol. **75.** (J. Hughes, editor).

Inoue A. & Kogure T. (2016) High-angle annular dark field scanning transmission electron microscopic (HAADF-STEM) study of Fe-rich 7 Å–14 Å interstratified minerals from a hydrothermal deposit. *Clay Minerals*, **51**, 603–613.

Inoue A., Meunier A., Patrier-Mas P., Rigault C., Beaufort D. & Vieillard P. (2009) Application of chemical geothermometry to low-temperature trioctahedral chlorites. *Clays and Clay Minerals*, **57**, 371–382.

Inoue A., Kurokawa K. & Hatta T. (2010) Application of chlorite geothermometry to hydrothermal alteration in Toyoha geothermal system, southwestern Hokkaido, Japan. *Resource Geology*, **60**, 52–70.

Joswig W. & Fuess H. (1990) Refinement of a one-layer triclinic chlorite. *Clays and Clay Minerals*, **38**, 216–218.

Jung H. (1931) Untersuchungen über den Chamosit von Schmiedefeld I. Thüringen. *Cheme der Erde*, **6**, 275–306.

Jung H. & Köhler E. (1930) Untersuchungen über den Thuringit von Schmiedefeld in Thüringen. *Chemie der Erde*, **5**, 182.

Kawano M. & Tomita K. (1991) Mineralogy and genesis of clays in postmagmatic alteration zones, Makurazaki volcanic area, Kagoshima prefecture, Japan. *Clays and Clay Minerals*, **39**, 597–608.

Kimbara K. & Nagata H. (1974) Clay minerals in the core samples of the mineralized zone of Niida, southern part of Odate Akita Prefecture, Japan. *Japanese Association of Mineralogists, Petrologists and Economic Geologists Journal*, **69**, 239–254.

Kimbara K. & Sudo T. (1973) Chloritic clay minerals in tuffaceous sandstone of the Miocene Green Tuff formation, Yamanaka district, Ishikawa Prefecture, Japan. *Japanese Association of Mineralogists, Petrologists and Economic Geologists Journal*, **68**, 246–258.

Kimbara K., Shimoda S. & Sudo T. (1973) An unusual chlorite as revealed by the high temperature X-ray diffractometer. *Clay Minerals*, **10**, 71–78.

Kittrick J.A. (1982) Solubility of two high-Mg and two high-Fe chlorites using multiple equilibria. *Clays and Clay Minerals*, **30**, 167–179.

Kodama H., Longworth G. & Townsend M.G. (1982) A Mössbauer investigation of some chlorites and their oxidation products. *The Canadian Mineralogist*, **20**, 585–592.

Kramm U. (1980) Sudoite in low-grade metamorphic manganese rich assemblages. *Neues Jahrbuch für Mineralogie Abhandlungen*, **138**, 1–13.

Lanari P., Wagner T. & Vidal O. (2014a) A thermodynamic model for di-trioctahedral chlorite from experimental and natural data in the system MgO–FeO–Al_2O_3–SiO_2–H_2O: applications to P–T sections and geothermometry. *Contributions to Mineralogy and Petrology*, **167**, 1–19.

Lanari P., Vidal O., De Andrade V., Dubacq B., Lewin E., Grosch E.G. & Schwartz S. (2014b) XMapTools: A MATLAB©-based program for electron microprobe X-ray image processing and geothermobarometry. *Computers and Geosciences*, **62**, 227–240.

Lapham D.M. (1958) Structural and chemical variation in chromium chlorite. *American Mineralogist*, **43**, 921–956.

Laird J. (1988) Chlorites; metamorphic petrology. Pp. 405–453 in: *Hydrous Phyllosilicates (exclusive of Micas)* (S.W. Bailey, editor). Reviews in Mineralogy, **19**, Mineralogical Society of America, Washington, D.C.

Lazarenko E.K. (1940) Donbassites, a new group of minerals from the Donetz Basin. *CR Academy Science URSS*, **28**, 519–521.

Lin C.Y. & Bailey S.W. (1985) Structural data for sudoite. *Clays and Clay Minerals*, **33**, 410–414.

Lougear A., Grodzicki M., Bertoldi C., Trautwein A.X., Steiner K. & Amthauer G. (2000) Mössbauer and molecular orbital study of chlorites. *Physics and Chemistry of Minerals*, **27**, 258–269.

MacKenzie K.J.D. & Bowden M.E. (1983) Thermal and Mössbauer studies of iron-containing hydrous silicates. IV. Amesite. *Thermochimica Acta*, **64**, 83–106.

Malmström M., Banwart S., Lewenhagen J., Duro L. & Bruno J. (1996) The dissolution of biotite and chlorite at 25°C in the near-neutral pH region. *Journal of Contaminant Hydrology*, **21**, 201–213.

Malysheva T.V., Satarova L.M. & Polyakova N.P. (1977) Thermal transformations of layered silicates and the nature of the iron-bearing phase in the CII type Murray carbonaceous chondrite. *Geokhimiya*, **8**, 1136–1148.

Mathias M. (1952) A note on two actinolites and a chlorite from the Prieska district, Cape Province. *Transactions and Proceedings of the Geological Society of South Africa*, **55**, 13–18.

May H.M., Acker J.G., Smyth J.R., Bricker O.P. & Dyar M.D. (1995) Aqueous dissolution of low-iron chlorite in dilute acid solutions at 25 C. *Clay Minerals Society Proceedings, Abstract*, **32**, p. 88.

Mélon J. (1938) *Description des Chlorites et Clintonites Belges.* Palais des Académies, France.

Meunier A. (2005) *Clays.* Springer Science & Business Media, Berlin, 490 pp.

Mitra S. & Bidyananda M. (2001) Crystallo-chemical characteristics of chlorites from the greenstone belt of south India, and their geothermometric significance. *Clay Science*, **11**, 479–501.

Muñoz M., De Andrade V., Vidal O., Lewin E., Pascarelli S. & Susini J. (2006) Redox and speciation micromapping using dispersive X-ray absorption spectroscopy: Application to iron chlorite mineral of a metamorphic rock thin section. *Geochemistry Geophysics Geosystems*, **7**, Doi: 10.1029/2006GC001381.

Nakamura T. (1960) On chlorite from the Ashio copper mine, Japan. *Minerals Journal*, **4**, 383–397.

Nockholds S.R. & Richey J.E. (1939) Replacement veins in the Mourne Mountains granites, N. Ireland. *American Journal of Science*, **237**, 27–47.

Orcel J. (1927) *Recherches sur la Composition Chimique des Chlorites.* Société Générale d'Imprimerie et d'édition, France.

Pal T., Maity P.K., Das D. & Mitra S. (1993) Oxidation character of chlorite from Byrapur chromite deposit, India — An ^{57}Fe Mössbauer evaluation. *Bulletin of Materials Science*, **16**, 229–237.

Phillips T.L., Loveless J.K. & Bailey S.W. (1980) Cr^{3+} coordination in chlorites: a structural study of ten chromian chlorites. *American Mineralogist*, **65**, 112–122.

Poitevin E. & Graham R.P.D. (1918) *Contributions to the Mineralogy of Black Lake Area, Quebec.* Government Printing Bureau, France.

Post J.L. & Plummer C.C. (1972) The chlorite series of Flagstaff Hill area, California: A preliminary investigation. *Clays and Clay Minerals,* **20**, 271–83.

Rigault C. (2010) *Cristallochimie du fer dans les chlorites de basse température: implications pour la géothermométrie et la détermination des paléoconditions redox dans les gisements d'uranium*. Thèse de doctorat, Université de Poitiers, France.

Ross C.S. (1935) *Origin of the Copper Deposits of the Ducktown Type in the southern Appalachian Region.* US Government Printing Office, USA.

Rule A.C. & Bailey S.W. (1987) Refinement of the crystal structure of a monoclinic ferroan clinochlore. *Clays and Clay Minerals*, **35**, 129–138.

Shannon E.V. & Wherry E.T. (1922) Notes on white chlorites. *Journal of the Washington Academy of Science*, **12**, 239.

Shimane H. & Sudo T. (1958) A chloritic mineral found associated with vermiculite. *Clay Minerals Bulletin*, **3**, 297–301.

Shimoda S. (1970) An expandable chlorite-like mineral from the Hanaoka Mine, Akita Prefecture, Japan. *Clay Minerals Bulletin*, **8**, 352–359.

Shirozu H. (1958) X-ray powder patterns and cell dimensions of some chlorites in Japan, with a note

on their interference colors. *Mineralogical Journal*, **2**, 209–223.

Simpson E.S. (1936) Contributions to the mineralogy of Western Australia. *Royal Society of Western Australia Journal*, **22**, 1–18.

Simpson E.S. (1937) Contributions to the mineralogy of Western Australia. *Royal Society of Western Australia Journal*, **23**, 17–35.

Singer D.M., Maher K. & Brown G.E. Jr (2009) Uranyl–chlorite sorption/desorption: Evaluation of different U(VI) sequestration processes. *Geochimica et Cosmochimica Acta*, **73**, 5989–6007.

Smyth J.R., Dyar M.D., May H.M., Bricker O.P. & Acker J.G. (1997) Crystal structure refinement and Mössbauer spectroscopy of an ordered, triclinic clinochlore. *Clays and Clay Minerals*, **45**, 544–550.

Spanu V., Filoti G., Ionescu J. & Medesan A. (1977) Mössbauer study of some chlorites. In: *Proceedings of the International Conference on Mössbauer Spectroscopy*, Editorial Group of the Revue Roumaine de Physique, Bucharest, pp. 323–324.

Stone R.L. & Weiss E.J. (1955) Examination of four coarsely crystalline chlorites by X-ray and high-pressure DTA techniques. *Clay Minerals Bulletin*, **2**, 214–222.

Sudo T. & Shimoda S. (1978) *Clays and Clay Minerals of Japan*, Vol. 26. Elsevier.

Tilley C.E. (1938) The status of hornblende in low-grade metamorphic zones of green schists. *Geological Magazine*, **75**, 497–511.

Trincal V., Lanari P., Buatier M., Lacroix B., Charpentier D., Labaume P. & Muñoz M. (2015) Temperature micro-mapping in oscillatory-zoned chlorite: Application to study of a greenschist facies fault zone in the Pyrenean Axial Zone (Spain). *American Mineralogist*, **100**, 2468–2483.

Tschermak G. (1891) *Die Chloritgruppe.* Sitzungberichte Akademie der Wissenschaften, Wien, **100**, 29 pp.

Tsukahara N. (1964) Dioctahedral chlorite from the Furutobe mine, Akita prefecture, Japan. *Clay Science*, **2**, 56–75.

Tsuzuki Y. & Honda S. (1977) Three examples of Mg-Al chlorite from Kuroko deposits. *Journal of the Mineralogical Society of Japan*, **13**, 85–93.

Vidal O., Parra T. & Trotet F. (2001) A thermodynamic model for Fe-Mg aluminous chlorite using data from phase equilibrium experiments and natural pelitic assemblages in the 100 degrees to 600 degrees C, 1 to 25 kb range. *American Journal of Science*, **301**, 557–592.

Vidal O., Parra T. & Vieillard P. (2005) Thermodynamic properties of the Tschermak solid solution in Fe-chlorite: Application to natural examples and possible role of oxidation. *American Mineralogist*, **90**, 347–358.

Vidal O., De Andrade V., Lewin E., Muñoz M., Parra T. & Pascarelli S. (2006) P-T-deformation-Fe^{3+}/Fe^{2+} mapping at the thin section scale and comparison with XANES mapping: application to a garnet-bearing metapelite from the Sambagawa metamorphic belt (Japan). *Journal of Metamorphic Geology*, **24**, 669–683.

Vidal O., Lanari P., Munoz M., Bourdelle F. & de Andrade V. (2016) Deciphering temperature, pressure and oxygen activity conditions of chlorite formation. *Clay Minerals*, **51**, 615–633.

Vrublevskaja Z.V., Delitsin I.S., Zvyagin B.B. & Soboleva S.V. (1975) Cookeite with a perfect regular structure, formed by bauxite alteration. *American Mineralogist*, **60**, 1041–1046.

Weaver C.E., Wampler J.M. & Pecuil T.E. (1967) Mössbauer analysis of iron in clay minerals. *Science*, **156**, 504–508.

Wiewióra A. & Weiss Z. (1990) Crystallochemical classifications of phyllosilicates based on the unified system of projection of chemical composition; II. The chlorite group. *Clay Minerals*, **25**, 83–92.

Wilke M., Farges F., Petit P.-E., Brown G.E. & Martin F. (2001) Oxidation state and coordination of Fe in minerals: An Fe K-XANES spectroscopic study. *American Mineralogist*, **86**, 714–730.

Zazzi A., Hirsch T.K., Leonova E., Kaikkonen A., Grins J., Annersten H. & Edén M. (2006) Structural investigations of natural and synthetic chlorite minerals by X-ray diffraction, Mössbauer spectroscopy and solid-state nuclear magnetic resonance. *Clays and Clay Minerals*, **54**, 252–265.

Zhang G., Burgos W.D., Senko J.M., Bishop M.E., Dong H., Boyanov M.I. & Kemner K.M. (2011) Microbial reduction of chlorite and uranium followed by air oxidation. *Chemical Geology*, **283**, 242–250.

Zheng H. & Bailey S.W. (1989) Structures of intergrown triclinic and monoclinic IIb chlorites from Kenya. *Clays and Clay Minerals*, **37**, 308–316.